Atmospheric Environment 51 (2012) 250–259

Contents lists available at SciVerse ScienceDirect

Atmospheric Environment

journal homepage: www.elsevier.com/locate/atmosenv

Characterization of summer organic and inorganic aerosols in Beijing, China with an Aerosol Chemical Speciation Monitor

Yele Sun [a,*], Zifa Wang [a,*], Huabin Dong [a], Ting Yang [a], Jie Li [a], Xiaole Pan [a], Ping Chen [b,c], John T. Jayne [d]

[a] State Key Laboratory of Atmospheric Boundary Layer Physics and Atmospheric Chemistry, Institute of Atmospheric Physics, Chinese Academy of Sciences, Beijing, China
[b] Nanjing University of Information Science and Technology, Nanjing, China
[c] Handix LLC, Boulder, CO, USA
[d] Aerodyne Research, Inc., Billerica, MA, USA

ARTICLE INFO

Article history:
Received 14 December 2011
Received in revised form
5 January 2012
Accepted 6 January 2012

Keywords:
ACSM
Particulate matter
Organic aerosol
Sources
Beijing

ABSTRACT

An Aerodyne Aerosol Chemical Speciation Monitor (ACSM) was first deployed in Beijing, China for characterization of summer organic and inorganic aerosols. The non-refractory submicron aerosol (NR-PM_1) species, i.e., organics, sulfate, nitrate, ammonium, and chloride were measured in situ at a time resolution of ~15 min from 26 June to 28 August, 2011. The total NR-PM_1 measured by the ACSM agrees well with the $PM_{2.5}$ measured by a Tapered Element Oscillating Microbalance (TEOM). The average total NR-PM_1 mass for the entire study is 50 ± 30 μg m^{-3} with the organics being the major fraction, accounting for 40% on average. High concentration and mass fraction of nitrate were frequently observed in summer in Beijing, likely due to the high humidity and excess gaseous ammonia that facilitate the transformation of HNO_3 to ammonium nitrate particles. Nitrate appears to play an important role in leading to the high particulate matter (PM) pollution since its contribution increases significantly as a function of aerosol mass loadings. Positive matrix factorization (PMF) of ACSM organic aerosol (OA) shows that the oxygenated OA (OOA) – a surrogate of secondary OA dominates OA composition throughout the day, on average accounting for 64%, while the hydrocarbon-like OA (HOA) shows a large increase at meal times due to the local cooking emissions. Our results suggest that high PM pollution in Beijing associated with stagnant conditions and southern air masses is characterized by the high contribution of secondary inorganic species and OOA from regional scale, whereas the aerosol particles during the clean events are mainly contributed by the local emissions with organics and HOA being the dominant contribution.

1. Introduction

Atmospheric aerosols, from a wide variety of natural and anthropogenic sources, are important components of atmosphere. Aerosol particles have a large impact on visibility reduction and air quality on scales ranging from local to regional (Watson, 2002), and play a significant role in climate change by altering the radiative balance of the Earth's atmosphere directly and indirectly (Forster et al., 2007). Aerosol particles, especially particles with small sizes, also exert a serious impact on human health causing the increase of respiratory and cardiovascular disease and reducing life expectancy (Pope et al., 2002, 2009). Thus, a comprehensive characterization of chemical composition, sources and evolution processes are essential for unraveling the complexity of particulate matter (PM) and evaluate its effects on climate and public health.

Rapid industrialization, urbanization, and economic growth have resulted in a substantial increase of anthropogenic emissions of aerosols and their precursors in China (Streets et al., 2003; Zhang et al., 2007b). Air pollution thus has become a major environmental concern, especially in megacities across the whole country (Chan and Yao, 2008). The concentrations of PM, especially fine particles ($PM_{2.5}$), often exceed the ambient air quality standards of US Environmental Protection Agency (15 μg m^{-3}, annual average) and the World Health Organization (10 μg m^{-3}, annual average). As a result, extensive efforts have been made during the last decade to characterize the sources, properties and processes of PM in China. The mass concentrations, chemical composition (elements, water-soluble ions, and elemental carbon (EC) and organic carbon (OC)), and sources of PM_{10} and $PM_{2.5}$ have been investigated in detail

* Corresponding authors. Tel.: +86 10 82013200; fax: +86 10 62041393.
E-mail addresses: sunyele@mail.iap.ac.cn (Y. Sun), zifawang@mail.iap.ac.cn (Z. Wang).

1352-2310/$ – see front matter © 2012 Elsevier Ltd. All rights reserved.
doi:10.1016/j.atmosenv.2012.01.013

(He et al., 2001; Yao et al., 2002; Sun et al., 2004; Duan et al., 2005; Wang et al., 2005; Zheng et al., 2005; Sun et al., 2006; Yang et al., 2010b). Carbonaceous material, sulfate, nitrate and ammonium have been found to comprise the major fraction of fine particles (Yang et al., 2011a). The sources of PM mainly include secondary inorganic species, coal combustion, vehicle exhaust, biomass burning, and mineral dust etc. depending on seasons and sites (Zheng et al., 2005; Song et al., 2006; Chan and Yao, 2008). However, most of previous studies are based on filter measurements which are limited by either a fixed site or a low time resolution from hours to days. The knowledge of the rapid evolution processing of aerosol components is not well known.

Aerodyne Aerosol Mass Spectrometer (AMS) is capable of providing size-resolved real-time measurements of non-refractory submicron aerosol (NR-PM_1) species (Jayne et al., 2000). AMS relying upon thermal vaporization (typically at 600 °C) and 70 eV electron-impact ionization (EI) (e.g., Canagaratna et al., 2007) has been widely used in both field measurements and chamber studies. The application of Aerodyne AMS in Beijing, China started in 2006 (Takegawa et al., 2009a; Sun et al., 2010a) followed by further deployments in 2008 (Huang et al., 2010; Zhang et al., 2011). The highly time- and size-resolved measurements offer us many valuable insights into the characteristics, sources and processes of submicron aerosols in Beijing. However, most of these studies are limited by a short sampling period, typically less than 2 months, due to the high cost and complexity of maintenance. Long-term measurements of aerosol composition and mass concentration are rather limited, yet important for a full understanding of aerosol characteristics in China. Aerodyne Aerosol Chemical Speciation Monitor (ACSM) built upon AMS is specially designed recently for long-term continuous measurements of the mass concentrations and composition of NR-PM_1 species (Ng et al., 2011). The performances of ACSM have been evaluated in detail during the Queens College Study in New York City in 2009 (Ng et al., 2011; Sun et al., 2011b). The eight weeks, continuous and unattended ACSM measurements showed good agreements with the measurements by a High-Resolution Time-of-Flight AMS (HR-AMS) and other collocated instruments.

In the present study, we first deploy an ACSM in Beijing, China for a long-term routine measurement of NR-PM_1 species including organics, sulfate, nitrate, ammonium, and chloride. Here, we report the results from the first two month measurements during 26 June–28 August, 2011 and demonstrate the capability of ACSM for real-time quantification of mass concentrations and composition of aerosol species in highly polluted environment. Insights into the sources, properties and evolution processes of summer aerosols in Beijing are presented. Positive matrix factorization (PMF) analysis of ACSM OA spectra, and the sources and processes of OA components are also discussed.

2. Experimental

2.1. Sampling site and meteorology

The submicron aerosol was measured *in-situ* from 26 June to 28 August, 2011 by the ACSM at Institute of Atmospheric Physics (IAP), Chinese Academy of Sciences (39°58′28″N, 116°22′16″E), which is located between the north 3rd and 4th ring road in Beijing. The sampling site is located on the roof of a second-story building (~8 m high), approximately 40 m from the nearest traffic road. The meteorology variables including temperature, relative humidity, wind speed, and wind direction were obtained from the meteorology tower of IAP, ~30 m from the sampling site. All the data in this study are reported at ambient temperature and pressure conditions in Beijing Standard Time.

2.2. Instrumentation and operation

Compared to previous versions of AMS (Jayne et al., 2000; Drewnick et al., 2005; DeCarlo et al., 2006), the ACSM uses the same aerosol sampling, and vaporization and ionization modules, but removes the size components, i.e., no size information. Without a chopper at the entrance of chamber, ACSM determines the particle and background signals by alternating the sample flow between ambient air and particle-free air which is controlled by a 3-way automated switching valve. In addition, a unique yet necessary design of ACSM is the internal naphthalene standard situated inside the chamber which can be used for the purposes of *m/z* calibration, ionization efficiency (IE) calibration, and ion transmission efficiency (TE) due to its intense parent ion peak *m/z* 128 but minor interferences on other fragment ions. The detailed descriptions of ACSM has been given in Ng et al. (2011). Briefly, aerosol particles with vacuum aerodynamic diameter (D_{va}) ~40–1000 nm are sampled into ACSM through a 100 μm critical orifice mounted at the inlet of an aerodynamic lens. The particles are then directed onto a resistively heated surface (~600 °C) where NR-PM_1 components are flash vaporized and ionized by 70 eV electron impact. The positive ions are then analyzed by a commercial quadrupole mass spectrometer.

Ambient aerosol was drawn inside the room through a ½ inch (outer diameter) stainless steel tube at a flow rate of ~3 L min^{-1}, of which ~84 cc min^{-1} was sub-sampled into the ACSM. An URG cyclone (Model: URG-2000-30ED) was supplied in front of the sampling inlet to remove coarse particles with a size cut-off of 2.5 μm. The residence time in the sampling tube is ~5 s. During this study, the ACSM was operated at a time resolution of ~15 min with a scan rate of mass spectrometer at 500 ms amu^{-1} from *m/z* 10 to 150.

The ACSM was calibrated for IE with ammonium nitrate following the procedures detailed in Ng et al. (2011). The monodispersed, size-selected 300 nm ammonium nitrate particles within a range of concentrations were sampled into both the ACSM and a condensation particle counter (CPC). IE was then determined by comparing the response factors of ACSM to the mass calculated with the known particle size and the number concentrations from CPC. Once the IE is determined, the changes of the internal standard naphthalene or air ions, e.g., *m/z* 28 (N_2^+) or *m/z* 32 (O_2^+) can be used to account for the degradation of detector. The naphthalene signal in the chamber is temperature dependent and needed to be corrected first using Clausius–Clapeyron equation (Ng et al., 2011). Note the variation of naphthalene signal cannot account for the change of flow rate while the air signals do.

The detection limits (DLs) of individual species for ACSM are determined as 3 times the standard deviation (3σ) of their mass concentrations in the particle-free ambient air. The DLs of organics, nitrate, sulfate, ammonium, and chloride for 30 min average data are 0.54, 0.06, 0.07, 0.25, and 0.03 μg m^{-3}, respectively. As ammonium shows similar DL to that reported in Ng et al. (2011), other species show overall higher DLs likely due to the different background signals.

A Tapered Element Oscillating Microbalance (TEOM series 1400a, Thermo Scientific) was simultaneously operated at the same site to measure the $PM_{2.5}$ mass at a time resolution of 1-min. In addition, a dual-wavelength (1064 nm and 532 nm) depolarization Lidar (National Institute for Environmental Studies, Japan) was operated on the roof of a second-story building at IAP, which is ~30 m from the sampling site. The detailed descriptions of Lidar instrument and operations are given in Yang et al. (2010a). The planetary boundary layer (PBL) height was then retrieved from the measurements at 532 nm with a cubic root gradient method (CRGM) developed by Yang et al. (submitted for publication).

2.3. Data analysis

The ACSM data were analyzed for the mass concentrations and composition with the standard ACSM data analysis software written in Igor Pro (WaveMetrics, Inc., Oregon USA). A collection efficiency (CE) was introduced to account for the incomplete detection of aerosol species, mainly due to particle bounce at the vaporizer (Matthew et al., 2008). For most ambient studies, CE = 0.5 is found to be representative with data uncertainties generally within ±20% (Canagaratna et al., 2007; Middlebrook et al., 2011). However, a high CE > 0.5 is observed when the aerosol particles are highly acidic or contain high fraction of ammonium nitrate or high content of particle phase water (Kleinman et al., 2007; Matthew et al., 2008). In this study, to reduce the uncertainties of CE due to particle phase water, a silica gel diffusion dryer was introduced to keep the relative humidity in sampling line below 40%. In addition, the aerosol particles in Beijing are overall neutralized (Huang et al., 2010; Sun et al., 2010a), particle acidity thus plays minor roles in affecting CE. The composition-dependent CE is mainly driven by the mass fraction of ammonium nitrate (ANMF), and the relationship between CE and ANMF can be parameterized as CE = max(0.45, 0.0833 + 0.9167 × ANMF) (Middlebrook et al., 2011). Given high fraction of ammonium nitrate is often observed in this study, variable CEs calculated using the equation above are applied. The ion TE corrections are also needed to calculate the mass concentrations since the TE decreases sharply as a function of *m/z*. Here we use the measured time-dependent TE from naphthalene fragment ion peaks with intensities >~1% for the correction, which has been shown to agree reasonably with those determined from the noble gases (Ng et al., 2011).

The PMF with PMF2.exe algorithm (v 4.2) (Paatero and Tapper, 1994) was performed on ACSM OA mass spectra following the procedures described in Ulbrich et al. (2009). Only *m/z* < 120 was used for PMF analysis due to the following reasons: 1) the signals above *m/z* > 120 account for a minor fraction of total signal, 2) the *m/z*'s > 120 have larger uncertainties because of low ion TE and the large interferences of naphthalene signals on some *m/z*'s (e.g., *m/z* 127, 128, and 129). The PMF2 solutions were then investigated with an Igor Pro-based PMF Evaluation Tool (PET, v 2.04) (Ulbrich et al., 2009). The time series, diurnal cycles, mass spectra, and correlations with external tracers are carefully evaluated. The solution of two components including a hydrocarbon-like OA (HOA) and an oxygenated OA (OOA) were chosen in this study.

3. Results and discussion

3.1. Submicron aerosol mass

Fig. 1a shows the time series of mass concentrations of NR-PM_1 measured by the ACSM and $PM_{2.5}$ by the TEOM. The total NR-PM_1 (=sulfate + nitrate + organics + ammonium + chloride) shows an overall similar trend to $PM_{2.5}$ (r^2 = 0.68). On average, NR-PM_1 reports 64% of the TEOM $PM_{2.5}$ mass, mainly because the ACSM only detects PM_1 and does not respond to refractory components such as black carbon and crustal materials. Our results are consistent with the observations by Zhang et al. (2011) in summer 2008 in Beijing that AMS NR-PM_1 species of sulfate, nitrate, and ammonium on average reported 56–61% of $PM_{2.5}$. Similarly, the water-soluble inorganic species (SO_4^{2-}, NO_3^-, NH_4^+, and Cl^-) measured by a Q-AMS agreed with those determined from five-stage Berner cascade impactor samples, and AMS PM_1 species reported

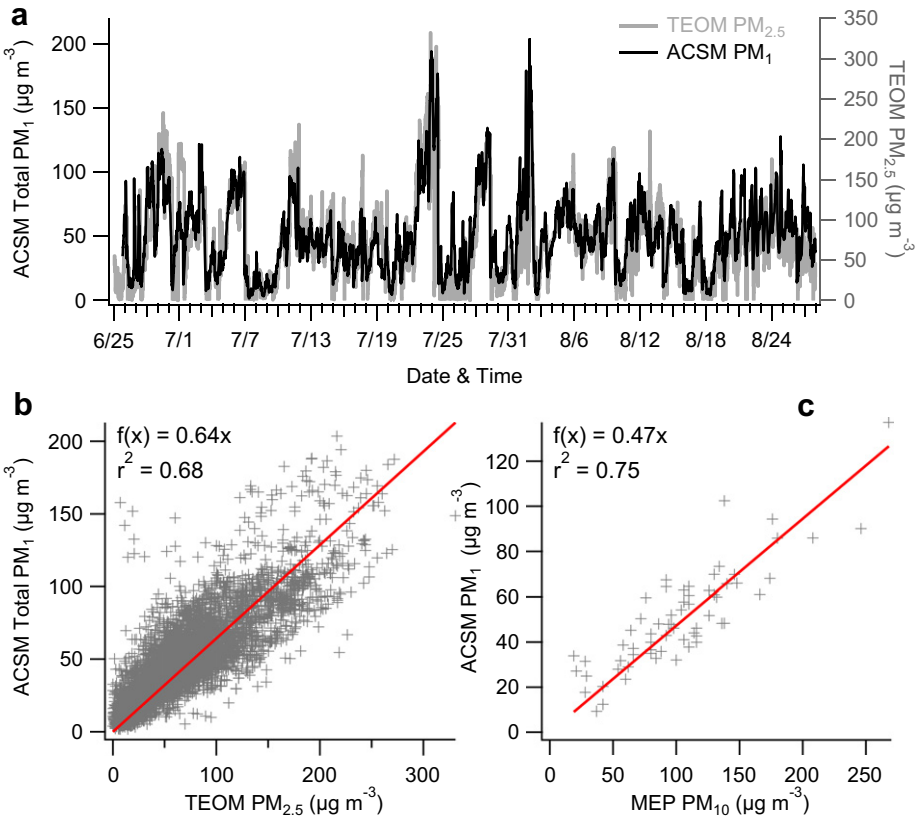

Fig. 1. (a) Time series of NR-PM_1 measured by the ACSM and $PM_{2.5}$ measured by the TEOM, (b) scatter plot of NR-PM_1 versus $PM_{2.5}$, and (c) scatter plot of daily average NR-PM_1 versus PM_{10} reported by the Ministry of Environmental Protection (MEP) of the People's Republic of China.

~61–87% of those in $PM_{1.2}$ (Takegawa et al., 2009b). Fig. 1c presents a comparison of daily average of NR-PM_1 with PM_{10} calculated from the air pollution index (API) that was reported by the Ministry of Environmental Protection (MEP) of the People's Republic of China (http://datacenter.mep.gov.cn/). Again, the two measurements agree well and ACSM NR-PM_1 reports 47% on average of PM_{10}, indicating that submicron aerosol mass accounts for a large fraction of inhalable particulate matter in Beijing.

The average ($\pm 1\sigma$) NR-PM_1 mass for the entire study is 50 ($\pm$30) μg m^{-3} with hourly average ranging from 2.3 to 190 μg m^{-3}. In comparison to the measured NR-PM_1 mass at the Chinese Academy of Meteorological Sciences (CAMS) in 2006 by a Q-AMS (80 ± 41 μg m^{-3}) (Sun et al., 2010a) and at the Peking University (PKU) in 2008 by a HR-AMS (61.3 μg m^{-3}) (Huang et al., 2010), the submicron aerosol mass appears to show a decreasing trend during the past several years, consistent with the decreasing trend of aerosol optical depth (AOD) in August from 2006 to 2010 in Beijing (Xue et al., 2011). Another reason for the lower submicron mass is due to the much higher amount of precipitation in 2011 than previous years, which often scavenges the hygroscopic aerosol species efficiently (Sun et al., 2011a). Given that the average total NR-PM_1 mass might vary because of the different sampling dates, we further compared the total NR-PM_1 mass measured during the same sampling period among different years. The average NR-PM_1 mass during 9–21 July in 2011 is 40 ± 18 μg m^{-3}, twice lower than 80 μg m^{-3} observed during the same sampling period in 2006. In contrast, the average NR-PM_1 mass of 53 ± 32 μg m^{-3} in 2011 is close to 51 ± 35 μg m^{-3} in 2008 during the same sampling period of 23 July–28 August. Note that the stringent measures for emission controls were implemented during 23 July–28 August, 2008, leading to a significant reduction of PM pollution. Despite this, the PM_1 mass is often several times higher than those observed in a number of megacities, e.g., New York City, Mexico City, and Tokyo etc. and tens of times higher than those reported at rural locations in the United States or Europe (Zhang et al., 2007a), thus continuous efforts to reduce the source emissions of PM are needed.

3.2. Mass concentrations and composition

Fig. 2 shows the time series of mass concentrations of NR species for the entire study. All aerosol species show very dynamic variations because of changes of source emissions, meteorology, PBL height, photochemical reactions and regional transport. The aerosol species were often observed to be rapidly built up under stagnant meteorological conditions (e.g., high humidity and low wind speed) over the course of several days (e.g., 22–25 July), or dramatically reduced because of the quick removal processes associated with heavy rain falls and/or the dilution of clean air masses from north or northwest (e.g., 29 July). Similar accumulation and cleaning processes of submicron aerosol species were also observed at a rural site Yufa in 2006 (Takegawa et al., 2009a). Overall, organics comprise the major fraction of PM_1, accounting for 40% on average, with the nitrate being the second largest. Nitrate and sulfate account for 25% and 18%, respectively, of the total NR-PM_1 mass, while chloride represents a minor fraction, ~1%. Table 1 presents a comparison of the average composition of NR-PM_1 between this study and 2006 and 2008. The average bulk composition of NR-PM_1 shows similar dominance of organics to previous observations in Beijing (Huang et al., 2010; Sun et al., 2010a), but lower mass concentrations for all species except nitrate. Sulfate shows the largest reduction by 55% since 2006, likely due to the decrease of SO_2 emissions during the past five years. The mass concentration of nitrate shows a large decrease in summer 2008, consistent with the significant reduction of NO_x because of the source emissions control during the Olympic Games (Yang et al., 2011b), but rebounds back in 2011 due to the increase of NO_x in recent years based on the Beijing Environmental Statement (http://www.bjepb.

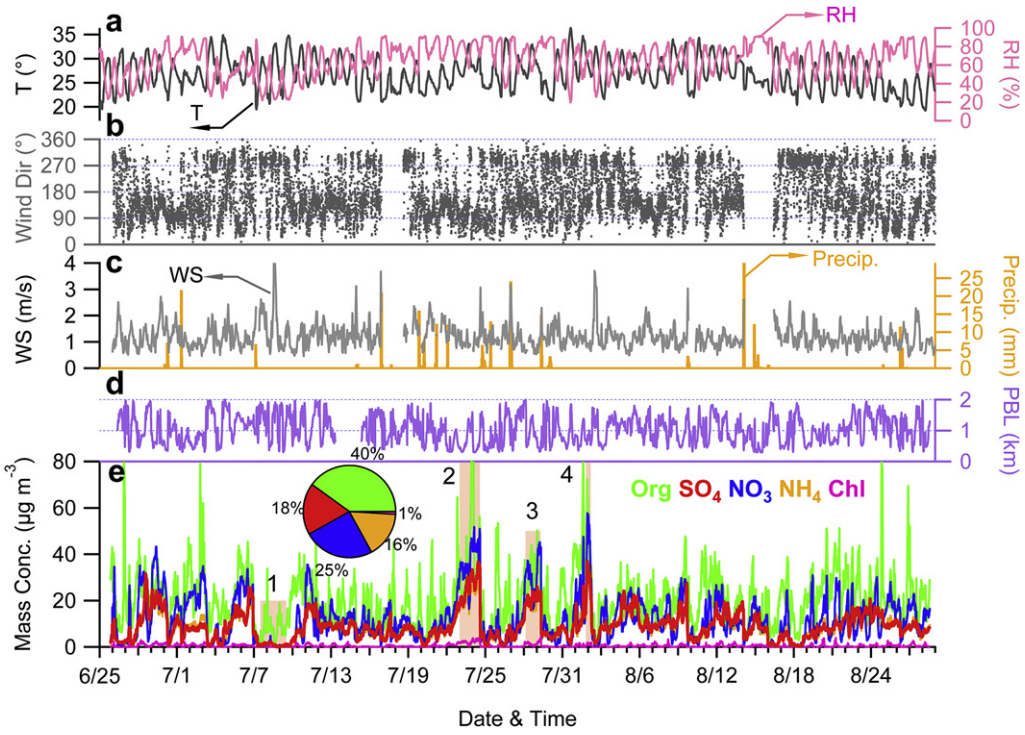

Fig. 2. Time series of (a) temperature (T) and relative humidity (RH); (b) wind direction; (c) wind speed (WS) and precipitation; (d) planetary boundary layer (PBL) height; and (e) submicron aerosol species, i.e., organics, sulfate, nitrate, ammonium, and chloride. The pie chart shows the average chemical composition of NR-PM_1 for the entire study. Four case events are marked and discussed in the text.

Table 1
Summary of mass concentrations (μg m^{-3}) and composition of NR-PM_1 species and OA components for the entire study and four case events as marked in Fig. 2. The AMS data measured at CAMS in July 2006 (Sun et al., 2010a) and at PKU in July–September 2008 (Huang et al., 2010) are also presented.

	Entire study	Case 1	Case 2	Case 3	Case 4	July, 2006	July–Sep., 2008
Org	20.0	8.3	38.5	31.4	52.0	28.1	23.9
SO_4	9.0	0.92	26.5	20.9	29.4	20.3	16.8
NO_3	12.4	0.77	37.3	31.0	44.0	17.3	10.0
NH_4	8.0	0.80	22.4	19.1	25.5	13.1	10.0
Chl	0.5	0.04	2.3	1.4	1.2	1.10	0.55
Total[a]	49.9	10.8	127.0	103.8	152.1	80.0	61.3
HOA	7.1	4.3	12.2	7.7	13.7	11.5	10.2[b]
OOA	12.7	4.1	23.7	22.1	37.0	16.6[c]	13.7[c]

[a] Total = Org + SO_4 + NO_3 + NH_4 + Chl.
[b] HOA here refers to the sum of traffic HOA and COA.
[c] OOA = OOA-1 + OOA-2 or SV-OOA + LV-OOA.

gov.cn/portal0/tab181/). It appears that the variations of secondary inorganic aerosol species are closely related to the emissions of their precursors. For instance, due to the increase of NO_2 emissions and the reduction of SO_2, the contribution of nitrate to NR-PM_1 is found to increase while that of sulfate decreases over time. Similar increase of NO_3^-/SO_4^{2-} ratio was also observed in 2009–2010 compared to previous years by investigating the water-soluble ions from filter measurements (Zhao et al., 2011).

It's interesting to note that a large amount of nitrate presents in submicron aerosol particles and often exceeds the concentration of sulfate in summer (Fig. 2). This is not typical since ammonium nitrate is volatile and tends to remain in the gas phase under high temperatures. For example, Ianniello et al. (2011) found ~83% loss of nitrate due to the evaporation from Teflon filters in summer. The diurnal variation of nitrate shows low concentration in the afternoon (Fig. 3a), which is also likely due to the evaporative loss. However, when the dilution effects by PBL are considered, the diurnal cycle of nitrate presents a pronounced noon peak (Fig. 3c), indicating that the evaporative loss cannot overcome the photochemical production of HNO_3 from the reactions of NO_2 + OH. High concentration of nitrate persists throughout the day (7.4–15.7 μg m^{-3}) with the contribution to the total NR-PM_1 being 17–31%. One reason for such substantial nitrate in summer is due to the abundant gaseous ammonia (NH_3) in the atmosphere (Meng et al., 2011) that can neutralize the HNO_3 to form NH_4NO_3 particles. This is consistent with the bulk neutralized aerosol particles in this study and previous observations in Beijing (Huang et al., 2010; Sun et al., 2010a). Another reason is due to the high relative humidity in summer which facilitates the dissolve of HNO_3 and NH_3 into aqueous phase and enhances the concentration of ammonium nitrate (Ianniello et al., 2011).

Fig. 4 shows the variations of the meteorology (RH, wind speed and PBL) and the mass fractions of NR-PM_1 species as a function of total NR-PM_1 mass. Meteorology plays an important role in causing the high PM pollution. In general, the high aerosol mass loadings are associated with high humidity, low wind speed and low PBL. As the total NR-PM_1 mass is above 50 μg m^{-3}, the relative humidity is consistently high at > ~65%, the wind speed keeps low at ~1 m s^{-1}, and the PBL height is generally below 1000 m (Fig. 4a–c). Organics dominate the total NR-PM_1 mass at low mass loadings (e.g., 63% on average at NR-PM_1 <20 μg m^{-3}) and its contribution decreases till ~30% at the mass loadings of ~150 μg m^{-3}. The similar dominance of organics at low PM loadings was also observed at the rural site Yufa (Takegawa et al., 2009a) and the urban site PKU (Huang et al., 2010). Note that the organics show elevated contribution at mass loadings >160 μg m^{-3}, mainly due to a few organic plumes from local emissions. The inorganic species of nitrate and chloride, however, show a reversed trend to organics as a function of aerosol mass loadings. The contribution of nitrate is elevated from ~10% at low mass loadings to ~30% at high mass loadings, and similarly,

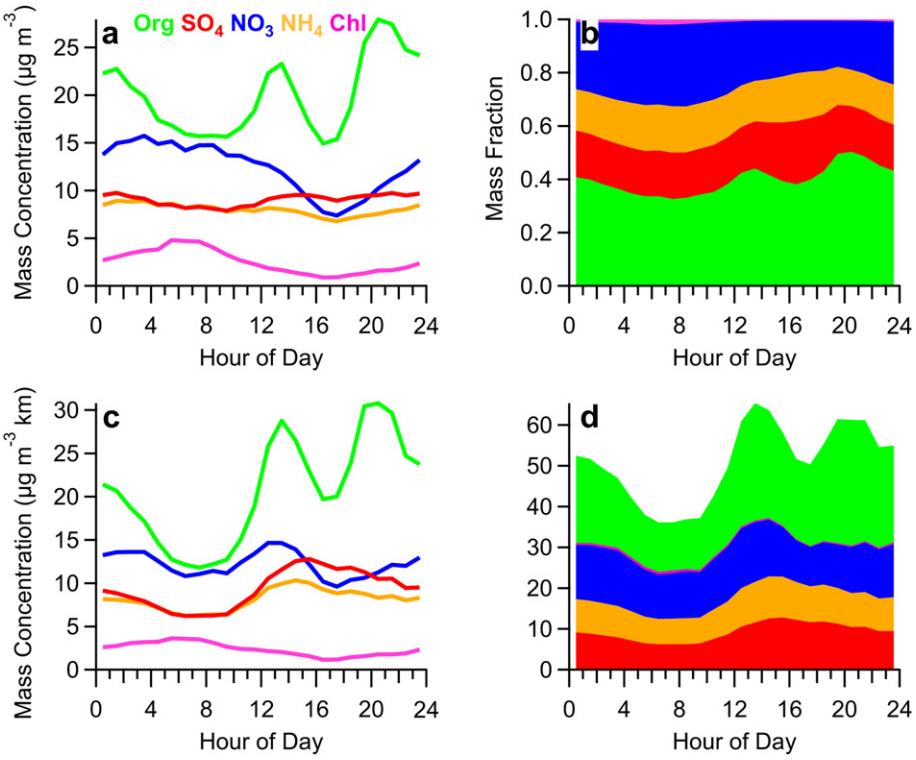

Fig. 3. Average diurnal cycles of (a) mass concentrations and (b) mass fraction, (c) planetary boundary layer (PBL) height normalized mass concentrations of NR-PM_1 species. (d) shows the stacked plot of diurnal cycle of PBL-normalized mass concentrations of NR-PM_1 species. The concentration of chloride in (a) and (c) is enhanced by a factor of 5 for clarity.

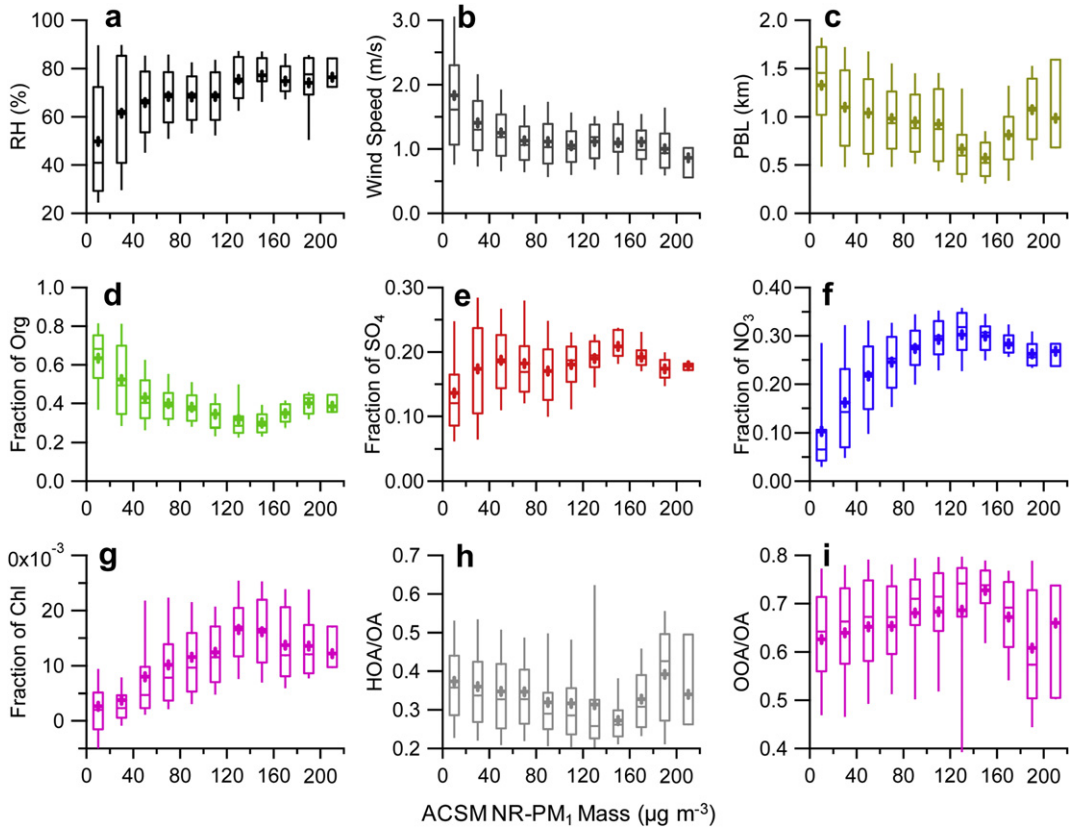

Fig. 4. (a) Relative humidity, (b) wind speed, (c) planetary boundary layer height, the mass fraction of (d) organics, (e) sulfate, (f) nitrate, and (g) chloride in NR-PM_1, and the mass fraction of (h) HOA and (i) OOA in OA as a function of NR-PM_1 mass loadings. The data were binned according to the total mass, and mean (cross), median (horizontal line), 25th and 75th percentiles (lower and upper box), and 10th and 90th percentiles (lower and upper whiskers) are shown for each bin.

the fraction of chloride is enhanced by a factor of 6 from 0.26% to 1.7%. It appears that ammonium nitrate and chloride play a more important role during the highly polluted events when the high humidity favors the partitioning of gas-phase species (e.g., HNO_3, NH_3, and HCl) to particles. Comparatively, sulfate remains a consistently high contribution ~15–20% across all the mass loadings. This finding might have important implications for the PM control strategy that reduction of the emissions of precursors of secondary inorganic species (e.g., SO_2 and NO_x) in Beijing would be effective to improve the air quality in Beijing, and also the measures should be implemented in both Beijing and surrounding regions.

3.3. Diurnal variations of NR species

Fig. 3 shows the average diurnal cycles of mass concentrations and composition of NR-PM_1 species. The organics present a pronounced diurnal cycle with two distinct peaks in the early afternoon (12:00–14:00) and in the evening (19:00–22:00). Similar diurnal patterns were also observed at CAMS in 2006and at PKU in 2008 (Huang et al., 2010; Sun et al., 2010a), and also other urban sites e.g., New York City, USA (Sun et al., 2011b) and London, UK (Allan et al., 2010). The contributions of organics to the total NR-PM_1 for the two peaks are correspondingly high, accounting for 44% and 50%, respectively. Evidence by investigating the diurnal cycles of OA components suggests that the two peaks occurring at meal times are mainly contributed by cooking-related activities (Allan et al., 2010; Huang et al., 2010; Sun et al., 2011b). Sulfate shows a flat diurnal cycle with a slight increase in the afternoon, similar to those observed in 2008 (Huang et al., 2010). This is consistent with the secondary nature of sulfate that is mainly produced in regional scale. In fact, the frequent observations of multi-day build-up (e.g., 22–25, July) signify the regional influences on sulfate concentration. However, if considering the dilution effects of PBL, sulfate shows a gradual increase starting from ~10:00 till ~16:00, and then remains at a high concentration level. The results indicate that the photochemical production of H_2SO_4 from $SO_2 + OH$ also have played an important role in driving the diurnal variation of sulfate. Both nitrate and chloride show similar diurnal cycles with the highest concentrations appearing in the early morning since these two species show similar volatile characteristics, and their concentrations are both sensitive to temperature and RH. The chloride measured by the ACSM is primarily NH_4Cl since ACSM does not detect the chloride salts (e.g., NaCl) at the vaporizer temperature of ~600 °C. The chloride concentration drops rapidly after the morning and stays at a low level for the whole afternoon, indicating that the diurnal pattern of chloride is mainly driven by the temperature dependent gas-particle partitioning of ammonium chloride. Further support is that chloride presents the similar diurnal cycle even though the PBL effect is considered (Fig. 3c). The gaseous HCl measured in the Pearl River Delta region showed high concentration during day time and presented an opposite diurnal pattern to water-soluble chloride, likely from the evaporation of NH_4Cl though the reaction between HNO_3 and sea salt might also have played a role (Hu et al., 2008). Comparatively, the decrease of nitrate during daytime is much smoother than chloride, whereas the diurnal cycle of PBL-normalized nitrate even shows a pronounced noon peak, which is due to the competing effects between the photochemical production of HNO_3 and the evaporative loss at high temperature.

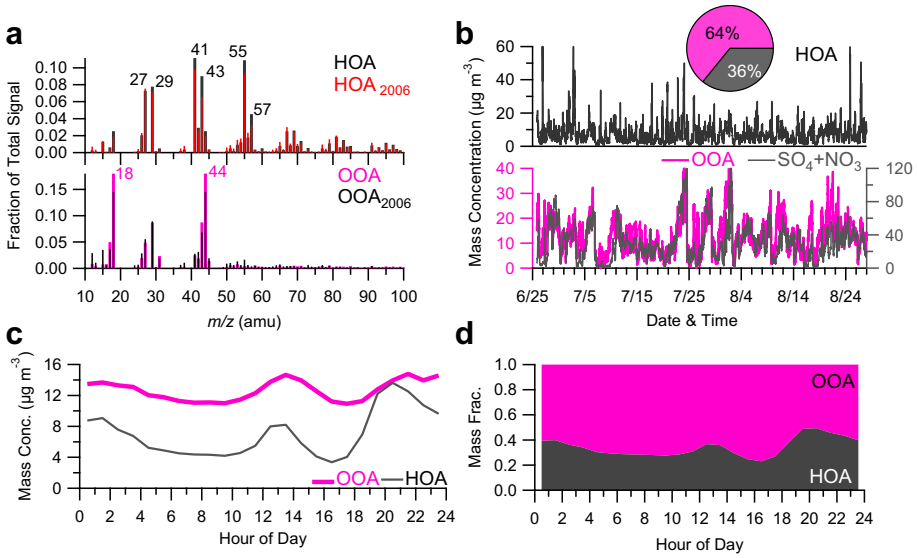

Fig. 5. (a) Mass spectra of HOA and OOA. The mass spectra of HOA and OOA-1 determined in 2006 (Sun et al., 2010a) are shown for a comparison; (b) time series of the mass concentrations of HOA, OOA, and secondary inorganic species (SO_4 + NO_3); (c, d) diurnal variations of the mass concentration and fractional contributions of HOA and OOA.

3.4. Investigation of OA components

PMF analysis of ACSM mass spectra of OA identified two components, i.e., HOA and OOA, each of which shows distinct time series and mass spectral profile corresponding to different sources and formation processes (Fig. 5). Increasing the number of factors leads to a third OA component that is mixed with HOA and OOA. Due to a lack of collocated measurements, only two components results are presented. The mass spectrum of HOA shows overall similarity to those of primary OA emitted from gasoline and diesel combustion sources (Canagaratna et al., 2004) and the spectra of HOA components determined at other urban sites (Zhang et al., 2005a; Allan et al., 2010; Sun et al., 2011b), all of which are characterized by the prominent hydrocarbon ion series of $C_nH^+_{2n-1}$ (e.g., *m/z* 27, 41, 55…) and $C_nH^+_{2n+1}$ (e.g., *m/z* 29, 43, 57…). Note that HOA in this study shows higher *m/z* 55/57 ratio in comparison to diesel exhaust aerosols, yet similar to the HOA component resolved in 2006 (r^2 = 0.97, Fig. 5a) (Sun et al., 2010a). High *m/z* 55/57 together with the unique diurnal variation has been used as a diagnostics for the presence of cooking OA (COA) (Mohr et al., 2009; Allan et al., 2010; Sun et al., 2011b), another primary OA (POA) component mainly from cooking activities. The diurnal cycle of HOA in this study shows two pronounced peaks corresponding to noon and evening meal times, indicating a large contribution of COA to POA. The results above suggest that HOA in this study is a mixture of traffic HOA and COA. In 2008, PMF analysis of high resolution mass spectra of OA was able to distinguish the COA from the traffic HOA (Huang et al., 2010). The mass spectrum of traffic HOA showed comparable signals of *m/z* 55 and 57, yet higher oxidation state (oxygen-to-carbon ratio, O/C = 0.15) than those from fresh vehicle emissions (~0.03–0.04) (Mohr et al., 2009). The traffic HOA accounted for 18% of total OA in 2008, slightly lower than that of COA (24%) (Huang et al., 2010). The HOA in this study from both traffic and cooking emissions on average contributes 36% of total OA for the entire study, similar to the contribution of POA (=HOA + COA) in 2006 (41%) (Jimenez et al., 2009) and 2008 (42%) (Huang et al., 2010).

The mass spectrum of OOA resembles to that of OOA-1 determined in 2006 in Beijing (Sun et al., 2010a) and OOA components resolved at other urban sites (Lanz et al., 2007; Ulbrich et al., 2009), which is characterized by a prominent peak at *m/z* 44 (mainly CO_2^+). OOA correlates well with secondary inorganic species (SO_4^{2-} + NO_3^-)

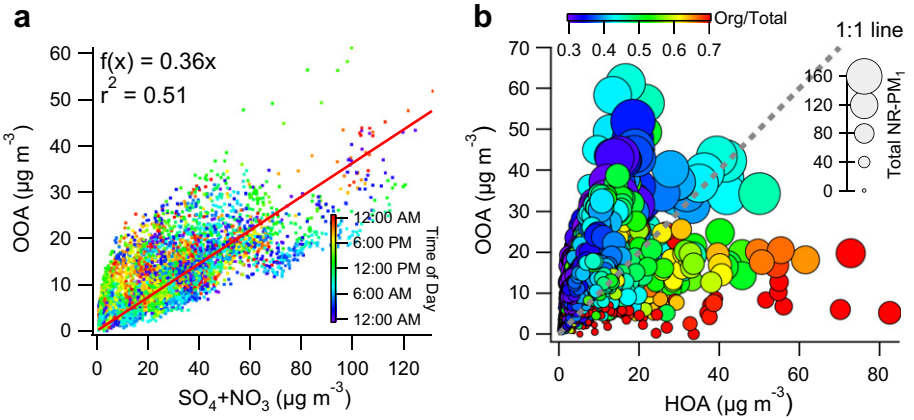

Fig. 6. (a) Correlation plot of OOA versus secondary inorganic species (SO_4+NO_3) colored by time of day; (b) correlation plot between OOA and HOA. The markers are colored by the mass fraction of organics in NR-PM_1 mass, and the marker sizes are proportional to the mass concentrations of NR-PM_1. (For interpretation of the references to color in this figure legend, the reader is referred to the web version of this article.)

(r^2 = 0.51, Fig. 6a), consistent with a conclusion achieved from a number of previous studies showing that OOA is secondary in nature and mostly driven by regional production (Zhang et al., 2005b; Kondo et al., 2007). Also, the ratio of OOA to secondary inorganic species ($SO_4^{2-} + NO_3^-$, 0.36, Fig. 6a) is close to 0.37–0.42 observed in 2006 and 2008 (Huang et al., 2010; Sun et al., 2010a; Zhang et al., 2011). The diurnal variation of OOA is relatively flat, but with an observable noon peak. Note that the appearance of OOA noon peak appears to be after the HOA noon peaks, likely due to the photochemical oxidation of semi-volatile organic species. OOA dominates OA composition throughout the whole day (51–77%). On average, OOA contributes 64% of OA, close to the values observed in previous years (Huang et al., 2010; Sun et al., 2010a). A correlation plot between OOA and HOA is shown in Fig. 6b. OOA and HOA shows weak correlations (r^2 = 0.24), confirming their different sources origins. However, a general trend is observed that the high PM pollution is associated with the elevated OOA but comparably low mass fraction of OA in NR-PM_1, while the low mass loadings are characterized by the dominant contribution of HOA from local traffic and cooking emissions. This is consistent with the increase of OOA contribution to total OA and a corresponding decrease of HOA as a function of total aerosol mass loadings as shown in Fig. 4.

3.5. Case studies of PM pollution

The relationship between the PM pollution, meteorology and chemical composition are further demonstrated by four case events (Table 1). High concentrations of NR species occupy most of time during this study, however, clean periods associated with north or northwest winds, low humidity, and high wind speeds are also observed, e.g., 7–9 July (Case 1). The back trajectories in Fig. 7 show that the air masses during Case 1 originated from the north and northwest of China, a clean region with low emissions of anthropogenic aerosols (Zhang et al., 2009; Sun et al., 2010b). The average concentration of total NR-PM_1 for this clean event is 10.8 μg m^{-3} with 77% being organics. PMF analysis shows that more than half of organics is primary particles from local traffic and cooking emissions. Comparatively, the other three typical pollution events on 23–24 July (Case 2), 28–29 July (Case 3), and 1–2 August (Case 4), respectively, are all characterized by high aerosol mass loadings

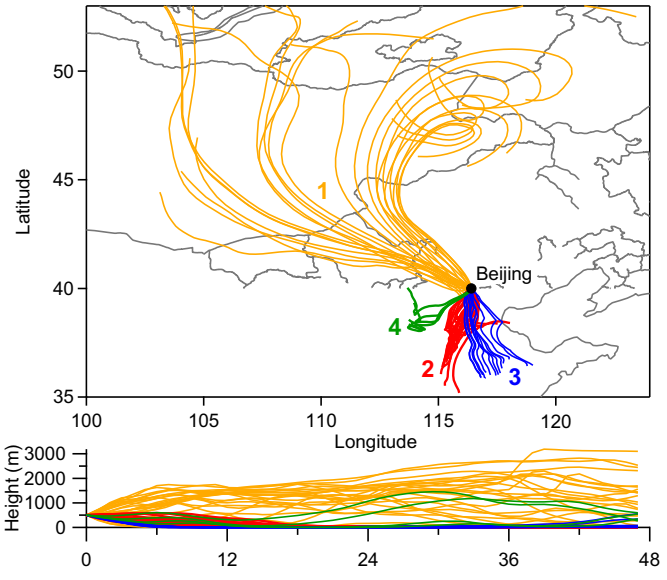

Fig. 7. Two-day back trajectories arriving at IAP, Beijing for the four case events marked in Fig. 2. The back trajectories at 500 m height were calculated every 2 h using NOAA HYSPLIT 4.8 model (Draxler and Rolph, 2003).

Table 2
Summary of meteorology for the four case events as marked in Fig. 2.

	Case 1	Case 2	Case 3	Case 4
Wind direction[a]	W, NW	E	S, SE, SW	SW
Wind speed (m s^{-1})	1.6	1.0	0.9	0.9
Temperature (°)	27.5	28.8	29.2	28.7
Relative humidity (%)	37	79	73	72

[a] W: west; NW: northwest; E: east; SE: southeast; SW: southwest.

(>100 μg m^{-3}). During the high PM pollution periods, the air masses mostly from the south, southeast or southwest are stagnant as suggested by the short trajectory distances. The wind speeds are correspondingly low (<1 m s^{-1}) and relative humidity is comparably high (>70%, Table 2). All these factors together result in the high PM pollution which often persists over a couple of days. The aerosol species are either continuously built up (Case 2) or remain at a high level (e.g., 11–14 July) till a change of the air masses or an interruption by the precipitation. The submicron aerosol composition during the high PM pollution periods is significantly different from that observed in the clean periods. Secondary inorganic species together accounts for ~70% of total NR-PM_1 mass, while organics contributes the rest of 30%. Similarly, secondary OA comprise the major fraction of OA (66–74%) indicating that regional production and transport plays a major role for the heavy pollution in summer in Beijing. Such composition-dependent evolution of PM pollution is typical in Beijing, which has been observed many times in previous studies (Takegawa et al., 2009a; Huang et al., 2010; Sun et al., 2010a). The results suggest again that controlling the secondary species from regional scale might be an effective way to improve the air quality in Beijing.

4. Conclusions

We first deployed an ACSM in Beijing, China for long-term routine measurements of non-refractory submicron aerosol species. For the two month study from 26 June to 28 August, 2011, ACSM shows good performances with the measured total NR-PM_1 in agreement with the $PM_{2.5}$ measured by the TEOM. The aerosol species vary very dynamically for the entire study. Multi-day build up under stagnant meteorological conditions or clean events due to rainfall scavenging or the dilution of clean air masses were frequently observed. Overall, organics comprise the major fraction, accounting for 40% on average, of total submicron aerosol mass. Compared to AMS measurements conducted in 2006 and 2008, we observed lower mass concentrations of total NR-PM_1 mass and all aerosol species except nitrate in summer 2011, likely due to the progresses in improving the air quality in Beijing and also the higher amount of precipitation during this year. An increase of ammonium nitrate contribution in submicron aerosols in comparison to previous years was observed, which likely reflects a change of source emissions, e.g., stationary vs. mobile sources in recent years. In addition, the photochemical production of HNO_3, which is facilitated to form ammonium nitrate particles under the conditions of high humidity and excess ammonia, plays an important role in driving the diurnal cycle of nitrate. PMF analysis was successfully applied to the ACSM OA spectra and was able to resolve two components, i.e., HOA and OOA. The mass spectra profiles and diurnal variations are consistent with those determined in previous AMS studies in Beijing, China. Taking the submicron aerosol species and OA components together, the high aerosol mass loadings are generally associated with the stagnant air masses and high humidity, and contributed dominantly by secondary inorganic species and OOA. This has an important implication for PM control strategy that priorities should be taken to control the emissions of

precursors of secondary species in Beijing as well as surrounding regions.

Acknowledgments

This study was supported by the National Natural Science Foundation of China (41175108), the Special Fund for Environmental Protection Research in the Public Interest (201009002), and Beijing Municipal Science and Technology Commission (D09040903670904). We thank the Technical and Service Center, Institute of Atmospheric Physics, Chinese Academy of Sciences for providing the meteorology data.

References

Allan, J.D., Williams, P.I., Morgan, W.T., Martin, C.L., Flynn, M.J., Lee, J., Nemitz, E., Phillips, G.J., Gallagher, M.W., Coe, H., 2010. Contributions from transport, solid fuel burning and cooking to primary organic aerosols in two UK cities. Atmos. Chem. Phys. 10, 647–668.

Canagaratna, M., Jayne, J., Jimenez, J.L., Allan, J.A., Alfarra, R., Zhang, Q., Onasch, T., Drewnick, F., Coe, H., Middlebrook, A., Delia, A., Williams, L., Trimborn, A., Northway, M., Kolb, C., Davidovits, P., Worsnop, D., 2007. Chemical and microphysical characterization of aerosols via Aerosol Mass Spectrometry. Mass Spectrom. Rev. 26, 185–222.

Canagaratna, M.R., Jayne, J.T., Ghertner, D.A., Herndon, S., Shi, Q., Jimenez, J.L., Silva, P.J., Williams, P., Lanni, T., Drewnick, F., Demerjian, K.L., Kolb, C.E., Worsnop, D.R., 2004. Chase studies of particulate emissions from in-use New York City vehicles. Aerosol Sci. Tech. 38, 555–573.

Chan, C.K., Yao, X., 2008. Air pollution in mega cities in China. Atmos. Environ. 42, 1–42. doi:10.1016/j.atmosenv.2007.09.003.

DeCarlo, P.F., Kimmel, J.R., Trimborn, A., Northway, M.J., Jayne, J.T., Aiken, A.C., Gonin, M., Fuhrer, K., Horvath, T., Docherty, K.S., Worsnop, D.R., Jimenez, J.L., 2006. Field-deployable, high-resolution, time-of-flight aerosol mass spectrometer. Anal. Chem. 78, 8281–8289.

Draxler, R.R., Rolph, G.D., 2003. HYSPLIT (HYbrid Single-Particle Lagrangian Integrated Trajectory) Model Access via NOAA ARL READY Website. NOAA Air Resources Laboratory, Silver Spring, MD. http://www.arl.noaa.gov/ready/hysplit4.html.

Drewnick, F., Hings, S.S., DeCarlo, P.F., Jayne, J.T., Gonin, M., Fuhrer, K., Weimer, S., Jimenez, J.L., Demerjian, K.L., Borrmann, S., Worsnop, D.R., 2005. A new time-of-flight aerosol mass spectrometer (ToF-AMS) – instrument description and first field deployment. Aerosol Sci. Tech. 39, 637–658.

Duan, F., He, K., Ma, Y., Jia, Y., Yang, F., Lei, Y., Tanaka, S., Okuta, T., 2005. Characteristics of carbonaceous aerosols in Beijing, China. Chemosphere 60, 355–364. doi:10.1016/j.chemosphere.2004.12.035.

Forster, P., Ramaswamy, V., Artaxo, P., Berntsen, T., Betts, R., Fahey, D.W., Haywood, J., Lean, J., Lowe, D.C., Myhre, G., Nganga, J., Prinn, R., Raga, G., Schulz, M., Dorland, R.V., 2007. Changes in atmospheric constituents and in radiative forcing. In: Solomon, S., Qin, D., Manning, M., Chen, Z., Marquis, M., Averyt, K.B., Tignor, M., Miller, H.L. (Eds.), Climate Change 2007: The Physical Science Basis. Contribution of Working Group I to the Fourth Assessment Report of the Intergovernmental Panel on Climate Change. Cambridge University Press, Cambridge, United Kingdom and New York, NY, USA.

He, K., Yang, F., Ma, Y., Zhang, Q., Yao, X., Chan, C.K., Cadle, S., Chan, T., Mulawa, P., 2001. The characteristics of $PM_{2.5}$ in Beijing, China. Atmos. Environ. 35, 4959–4970. doi:10.1016/s1352-2310(01)00301-6.

Hu, M., Wu, Z., Slanina, J., Lin, P., Liu, S., Zeng, L., 2008. Acidic gases, ammonia and water-soluble ions in $PM_{2.5}$ at a coastal site in the Pearl River Delta, China. Atmos. Environ. 42, 6310–6320. doi:10.1016/j.atmosenv.2008.02.015.

Huang, X.F., He, L.Y., Hu, M., Canagaratna, M.R., Sun, Y., Zhang, Q., Zhu, T., Xue, L., Zeng, L.W., Liu, X.G., Zhang, Y.H., Jayne, J.T., Ng, N.L., Worsnop, D.R., 2010. Highly time-resolved chemical characterization of atmospheric submicron particles during 2008 Beijing Olympic Games using an Aerodyne High-Resolution Aerosol Mass Spectrometer. Atmos. Chem. Phys. 10, 8933–8945. doi:10.5194/acp-10-8933-2010.

Ianniello, A., Spataro, F., Esposito, G., Allegrini, I., Hu, M., Zhu, T., 2011. Chemical characteristics of inorganic ammonium salts in $PM_{2.5}$ in the atmosphere of Beijing (China). Atmos. Chem. Phys. 11, 10803–10822. doi:10.5194/acp-11-10803-2011.

Jayne, J.T., Leard, D.C., Zhang, X., Davidovits, P., Smith, K.A., Kolb, C.E., Worsnop, D.R., 2000. Development of an aerosol mass spectrometer for size and composition analysis of submicron particles. Aerosol Sci. Tech. 33, 49–70.

Jimenez, J.L., Canagaratna, M.R., Donahue, N.M., Prevot, A.S.H., Zhang, Q., Kroll, J.H., DeCarlo, P.F., Allan, J.D., Coe, H., Ng, N.L., Aiken, A.C., Docherty, K.S., Ulbrich, I.M., Grieshop, A.P., Robinson, A.L., Duplissy, J., Smith, J.D., Wilson, K.R., Lanz, V.A., Hueglin, C., Sun, Y.L., Tian, J., Laaksonen, A., Raatikainen, T., Rautiainen, J., Vaattovaara, P., Ehn, M., Kulmala, M., Tomlinson, J.M., Collins, D.R., Cubison, M.J., Dunlea, E.J., Huffman, J.A., Onasch, T.B., Alfarra, M.R., Williams, P.I., Bower, K., Kondo, Y., Schneider, J., Drewnick, F., Borrmann, S., Weimer, S., Demerjian, K., Salcedo, D., Cottrell, L., Griffin, R., Takami, A., Miyoshi, T., Hatakeyama, S., Shimono, A., Sun, J.Y., Zhang, Y.M., Dzepina, K., Kimmel, J.R., Sueper, D., Jayne, J.T., Herndon, S.C., Trimborn, A.M., Williams, L.R., Wood, E.C., Middlebrook, A.M., Kolb, C.E., Baltensperger, U., Worsnop, D.R., 2009. Evolution of organic aerosols in the atmosphere. Science 326, 1525–1529. doi:10.1126/science.1180353.

Kleinman, L.I., Daum, P.H., Lee, Y., Senum, G.I., Springston, S.R., Wang, J., Berkowitz, C., Hubbe, J., Zaveri, R.A., Brechtel, F.J., 2007. Aircraft observations of aerosol composition and ageing in New England and Mid-Atlantic States during the summer 2002 New England Air Quality Study field campaign. J. Geophys. Res. 112, D09310. doi:09310.01029/02006JD007786.

Kondo, Y., Miyazaki, Y., Takegawa, N., Miyakawa, T., Weber, R., Jimenez, J., Zhang, Q., Worsnop, D.R., 2007. Oxygenated and water-soluble organic aerosols in Tokyo. J. Geophys. Res. 112, D01203. doi:01210.01029/02006JD007056.

Lanz, V.A., Alfarra, M.R., Baltensperger, U., Buchmann, B., Hueglin, C., Prévôt, A.S.H., 2007. Source apportionment of submicron organic aerosols at an urban site by factor analytical modelling of aerosol mass spectra. Atmos. Chem. Phys. 7, 1503–1522.

Matthew, B.M., Middlebrook, A.M., Onasch, T.B., 2008. Collection efficiencies in an Aerodyne Aerosol Mass Spectrometer as a function of particle phase for laboratory generated aerosols. Aerosol Sci. Tech. 42, 884–898.

Meng, Z.Y., Lin, W.L., Jiang, X.M., Yan, P., Wang, Y., Zhang, Y.M., Jia, X.F., Yu, X.L., 2011. Characteristics of atmospheric ammonia over Beijing, China. Atmos. Chem. Phys. 11, 6139–6151. doi:10.5194/acp-11-6139-2011.

Middlebrook, A.M., Bahreini, R., Jimenez, J.L., Canagaratna, M.R., 2011. Evaluation of composition-dependent collection efficiencies for the Aerodyne Aerosol Mass Spectrometer using field data. Aerosol Sci. Tech. 46, 258–271.

Mohr, C., Huffman, J.A., Cubison, M.J., Aiken, A.C., Docherty, K.S., Kimmel, J.R., Ulbrich, I.M., Hannigan, M., Jimenez, J.L., 2009. Characterization of primary organic aerosol emissions from meat cooking, trash burning, and motor vehicles with High-Resolution Aerosol Mass Spectrometry and comparison with ambient and chamber observations. Environ. Sci. Technol. 43, 2443–2449. doi:10.1021/es8011518.

Ng, N.L., Herndon, S.C., Trimborn, A., Canagaratna, M.R., Croteau, P.L., Onasch, T.B., Sueper, D., Worsnop, D.R., Zhang, Q., Sun, Y.L., Jayne, J.T., 2011. An Aerosol Chemical Speciation Monitor (ACSM) for routine monitoring of the composition and mass concentrations of ambient aerosol. Aerosol Sci. Tech. 45, 770–784.

Paatero, P., Tapper, U., 1994. Positive matrix factorization: a non-negative factor model with optimal utilization of error estimates of data values. Environmetrics 5, 111–126.

Pope, C.A., Burnett, R.T., Thun, M.J., Calle, E.E., Krewski, D., Ito, K., Thurston, G.D., 2002. Lung cancer, cardiopulmonary mortality, and long-term exposure to fine particulate air pollution. JAMA-J. Am. Med. Assoc. 287, 1132–1141.

Pope, C.A., Ezzati, M., Dockery, D.W., 2009. Fine-particulate air pollution and life expectancy in the United States. N. Engl. J. Med. 360, 376–386. doi:10.1056/NEJMsa0805646.

Song, Y., Zhang, Y., Xie, S., Zeng, L., Zheng, M., Salmon, L.G., Shao, M., Slanina, S., 2006. Source apportionment of $PM_{2.5}$ in Beijing by positive matrix factorization. Atmos. Environ. 40, 1526–1537. doi:10.1016/j.atmosenv.2005.10.039.

Streets, D.G., Bond, T.C., Carmichael, G.R., Fernandes, S.D., Fu, Q., He, D., Klimont, Z., Nelson, S.M., Tsai, N.Y., Wang, M.Q., 2003. An inventory of gaseous and primary aerosol emissions in Asia in the year 2000. J. Geophys. Res.-Atmos. 108 (D21), 8809. doi:8810.1029/2002JD003093.

Sun, J., Zhang, Q., Canagaratna, M.R., Zhang, Y., Ng, N.L., Sun, Y., Jayne, J.T., Zhang, X., Zhang, X., Worsnop, D.R., 2010a. Highly time- and size-resolved characterization of submicron aerosol particles in Beijing using an Aerodyne Aerosol Mass Spectrometer. Atmos. Environ. 44, 131–140.

Sun, Y., Zhuang, G., Huang, K., Li, J., Wang, Q., Wang, Y., Lin, Y., Fu, J., Zhang, W., Tang, A., Zhao, X., 2010b. Asian dust over northern China and its impact on the downstream aerosol chemistry in 2004. J. Geophys. Res. 115, D00K09. doi:10.1029/2009JD012757.

Sun, Y., Zhuang, G., Tang, A., Wang, Y., An, Z., 2006. Chemical characteristics of $PM_{2.5}$ and PM_{10} in haze-fog episodes in Beijing. Environ. Sci. Technol. 40, 3148–3155.

Sun, Y., Zhuang, G., Wang, Y., Han, L., Guo, J., Dan, M., Zhang, W., Wang, Z., Hao, Z., 2004. The air-borne particulate pollution in Beijing–concentration, composition, distribution and sources. Atmos. Environ. 38, 5991–6004.

Sun, Y.L., Zhang, Q., Schwab, J.J., Chen, W.N., Bae, M.S., Lin, Y.C., Hung, H.M., Demerjian, K.L., 2011a. A case study of aerosol processing and evolution in summer in New York City. Atmos. Chem. Phys. 11, 12737–12750.

Sun, Y.L., Zhang, Q., Schwab, J.J., Demerjian, K.L., Chen, W.N., Bae, M.S., Hung, H.M., Hogrefe, O., Frank, B., Rattigan, O.V., Lin, Y.C., 2011b. Characterization of the sources and processes of organic and inorganic aerosols in New York city with a high-resolution time-of-flight aerosol mass spectrometer. Atmos. Chem. Phys. 11, 1581–1602.

Takegawa, N., Miyakawa, T., Kuwata, M., Kondo, Y., Zhao, Y., Han, S., Kita, K., Miyazaki, Y., Deng, Z., Xiao, R., Hu, M., van Pinxteren, D., Herrmann, H., Hofzumahaus, A., Holland, F., Wahner, A., Blake, D.R., Sugimoto, N., Zhu, T., 2009a. Variability of submicron aerosol observed at a rural site in Beijing in the summer of 2006. J. Geophys. Res. 114, D00G05. doi:10.1029/2008jd010857.

Takegawa, N., Miyakawa, T., Watanabe, M., Kondo, Y., Miyazaki, Y., Han, S., Zhao, Y., van Pinxteren, D., Bruggemann, E., Gnauk, T., Herrmann, H., Xiao, R., Deng, Z., Hu, M., Zhu, T., Zhang, Y., 2009b. Performance of an Aerodyne Aerosol Mass Spectrometer (AMS) during intensive campaigns in China in the summer of 2006. Aerosol Sci. Tech. 43, 189–204.

Ulbrich, I.M., Canagaratna, M.R., Zhang, Q., Worsnop, D.R., Jimenez, J.L., 2009. Interpretation of organic components from Positive Matrix Factorization of aerosol mass spectrometric data. Atmos. Chem. Phys. 9, 2891–2918.

Wang, Y., Zhuang, G., Tang, A., Yuan, H., Sun, Y., Chen, S., Zheng, A., 2005. The ion chemistry and the source of $PM_{2.5}$ aerosol in Beijing. Atmos. Environ. 39, 3771–3784.

Watson, J.G., 2002. Visibility: science and regulation. J. Air Waste Manage. Assoc. 52, 628–713.

Xue, Y., Xu, H., Li, Y., Yang, L., Mei, L., Guang, J., Hou, T., He, X., Dong, J., Chen, Z., Qi, Y., 2011. Long-term aerosol optical depth datasets over China retrieved from satellite data. Atmos. Meas. Tech. Discuss. 4, 6643–6678. doi:10.5194/amtd-4-6643-2011.

Yang, F., Tan, J., Zhao, Q., Du, Z., He, K., Ma, Y., Duan, F., Chen, G., 2011a. Characteristics of $PM_{2.5}$ speciation in representative megacities and across China. Atmos. Chem. Phys. 11, 5207–5219. doi:10.5194/acp-11-5207-2011.

Yang, Q., Wang, Y., zhao, c., Liu, Z., Gustafson Jr., W.I., Shao, M., 2011b. NO_x emission reduction and its effects on ozone during the 2008 Olympic Games. Environ. Sci. Technol. 45, 6404–6410. doi:10.1021/es200675v.

Yang, T., Wang, Z., Zhang, B., Wang, X., Wang, W., Gbauidi, A., Gong, Y., 2010a. Evaluation of the effect of air pollution control during the Beijing 2008 Olympic Games using Lidar data. Chin. Sci. Bull. 55, 1311–1316. doi:10.1007/s11434-010-0081-y.

Yang, Y., Wang, Y., Huang, W., Hu, B., Wen, T., Zhao, Y., 2010b. Size distributions and elemental compositions of particulate matter on clear, hazy and foggy days in Beijing, China. Adv. Atmos. Sci. 27, 663–675.

Yang, T., Wang, Z.F., An, J.L., Su, D.B., Wang, X.Q., Zhang, W., Zhang, B., Gbaguidi, A., Wang, Z. A new method to estimate the planetary boundary layer height based on Lidar observations. SOLA, submitted for publication.

Yao, X., Chan, C.K., Fang, M., Cadle, S., Chan, T., Mulawa, P., He, K., Ye, B., 2002. The water-soluble ionic composition of $PM_{2.5}$ in Shanghai and Beijing, China. Atmos. Environ. 36, 4223–4234. doi:10.1016/s1352-2310(02)00342-4.

Zhang, Q., Alfarra, M.R., Worsnop, D.R., Allan, J.D., Coe, H., Canagaratna, M.R., Jimenez, J.L., 2005a. Deconvolution and quantification of hydrocarbon-like and oxygenated organic aerosols based on aerosol mass spectrometry. Environ. Sci. Technol. 39, 4938–4952. doi:4910.1021/es048568l.

Zhang, Q., Jimenez, J.L., Canagaratna, M.R., Allan, J.D., Coe, H., Ulbrich, I., Alfarra, M.R., Takami, A., Middlebrook, A.M., Sun, Y.L., Dzepina, K., Dunlea, E., Docherty, K., DeCarlo, P.F., Salcedo, D., Onasch, T., Jayne, J.T., Miyoshi, T., Shimono, A., Hatakeyama, S., Takegawa, N., Kondo, Y., Schneider, J., Drewnick, F., Weimer, S., Demerjian, K., Williams, P., Bower, K., Bahreini, R., Cottrell, L., Griffin, R.J., Rautiainen, J., Sun, J.Y., Zhang, Y.M., Worsnop, D.R., 2007a. Ubiquity and dominance of oxygenated species in organic aerosols in anthropogenically-influenced northern hemisphere mid-latitudes. Geophys. Res. Lett. 34, L13801. doi:10.1029/2007GL029979.

Zhang, Q., Streets, D.G., Carmichael, G.R., He, K.B., Huo, H., Kannari, A., Klimont, Z., Park, I.S., Reddy, S., Fu, J.S., Chen, D., Duan, L., Lei, Y., Wang, L.T., Yao, Z.L., 2009. Asian emissions in 2006 for the NASA INTEX-B mission. Atmos. Chem. Phys. 9, 5131–5153. doi:10.5194/acp-9-5131-2009.

Zhang, Q., Streets, D.G., He, K., Wang, Y., Richter, A., Burrows, J.P., Uno, I., Jang, C.J., Chen, D., Yao, Z., Lei, Y., 2007b. NO_x emission trends for China, 1995–2004: the view from the ground and the view from space. J. Geophys. Res. 112, D22306. doi:10.1029/2007jd008684.

Zhang, Q., Worsnop, D.R., Canagaratna, M.R., Jimenez, J.L., 2005b. Hydrocarbon-like and oxygenated organic aerosols in Pittsburgh: insights into sources and processes of organic aerosols. Atmos. Chem. Phys. 5, 3289–3311.

Zhang, Y.M., Zhang, X.Y., Sun, J.Y., Lin, W.L., Gong, S.L., Shen, X.J., Yang, S., 2011. Characterization of new particle and secondary aerosol formation during summertime in Beijing, China. Tellus B 63, 382–394. doi:10.1111/j.1600-0889.2011.00533.x.

Zhao, P., Zhang, X., Meng, W., Yang, B., Fan, W., Liu, H., 2011. Characteristics of inorganic water-soluble ions from aerosols in Beijing-Tianjin-Hebei Area. Environ. Sci. 32, 1546–1549.

Zheng, M., Salmon, L.G., Schauer, J.J., Zeng, L., Kiang, C.S., Zhang, Y., Cass, G.R., 2005. Seasonal trends in $PM_{2.5}$ source contributions in Beijing, China. Atmos. Environ. 39, 3967–3976. doi:10.1016/j.atmosenv.2005.03.036.